Intrinsic relaxation in a supercooled ZrTiNiCuBe glass forming liquid

N. Amini, F. Yang, E. Pineda, Beatrice Ruta, M. Sprung, A. Meyer

Intrinsic relaxation in a supercooled ZrTiNiCuBe glass forming liquid

N. Amini,[1] F. Yang,[1,*] E. Pineda,[2] B. Ruta,[3,4] M. Sprung,[5] and A. Meyer[1]

[1] *Institut für Materialphysik im Weltraum, Deutsches Zentrum für Luft- und Raumfahrt (DLR), 51170 Köln, Germany*
[2] *Department of Physics, Universitat Politècnica de Catalunya - BarcelonaTech, 08019 Barcelona, Spain*
[3] *Univ Lyon, Université Claude Bernard Lyon 1, CNRS, Institut Lumière Matière, 69622 Villeurbanne, France*
[4] *ESRF – The European Synchrotron, 71 avenue des Martyrs, 38000 Grenoble, France*
[5] *Deutsches Elektronen-Synchrotron (DESY), Notkestraße 85, Hamburg 22607, Germany*

(Dated: March 17, 2021)

We studied structural relaxation in the bulk metallic glass-forming alloy $Zr_{46.8}Ti_{8.2}Cu_{7.5}Ni_{10}$-$Be_{27.5}$ on different time and length scales, with emphasis on the supercooled liquid state. Using X-ray photon correlation spectroscopy, we determined the microscopic structural relaxation time covering timescales of more than two decades in the supercooled liquid region, down to sub-second regime. Upon heating across the glass transition, the intermediate scattering function changes from a compressed to a stretched decay, with a smooth transition in the stretching exponent and characteristic relaxation time. In the supercooled liquid state, the macroscopic and microscopic relaxation time, as well as the melt viscosity all exhibit the same temperature dependence. This points to a relaxation mechanism via intrinsic structural relaxation of the majority component Zr, with its microscopic timescale controlling both the stress relaxation and viscous flow of the melt.

I. INTRODUCTION

Metallic glasses (MGs) exhibit out-of-equilibrium disordered structure. As a consequence, their structural configurations permanently change towards a more stable state, a process called structural relaxation or physical aging [1]. The structural relaxation has been subjected to many experimental and theoretical investigations [2–6] due to its abundance of phenomenology, which is tightly connected with the structure and dynamics of glasses [7].

Due to the disordered structure, metallic glasses and bulk metallic glasses (BMGs) exhibit extraordinary physical and chemical properties, e.g.: high strength, high hardness, good corrosion and wear resistance, soft magnetic properties, etc [8–10]. This makes them attractive candidates for novel applications in many fields. Since the properties of the glass-forming melt are governed by the relaxational dynamics, knowledge of its timescales is not only essential for understanding fundamental processes like glass transition and transport phenomena, but also relevant for a range of technologically important processes related to MGs. For instance, the long range atomic transport, as well as macroscopic thermophysical properties like density and shear viscosity are key parameters during the fabrication of MGs, including additive manufacturing and thermoplastic molding [11, 12]. Also, the relaxation of metallic glasses towards a more stable (or aged) glassy state controls the long time evolution of their properties, which are crucial when used as structural materials [1].

BMGs provide a unique possibility for studying the structural relaxation behavior in both the glass and the supercooled liquid, owing to their good thermal stability against crystallization. In addition, compared to molecular or oxide glass formers, MGs are composed of atoms with no internal degrees of freedom, hence exhibit only translational dynamics. At elevated temperatures, close to the liquidus temperature, the dynamics of the melt exhibit a two-step structural relaxation, with the long-time, so-called α-relaxation dominated by highly coupled microscopic timescales [13, 14]. In contrast, at low temperatures close to the glass transition, the relaxation pathway is more complex and heterogeneous, with a number of secondary relaxation processes, decoupled from the primary α-relaxation [1, 15–17]. So far, these processes have been primarily probed mechanically on macroscopic scale [1, 15, 17], mainly by characterizing the creep behavior under static mechanical load, the stress relaxation under static deformation, or the mechanical response (moduli) to periodic strain oscillations as a function of frequency [15]. The timescales cover a range from 10^{-3} s to 10^{3} s, which correspond typically to the α- and β-relaxation processes in the glass and supercooled liquid regions.

However, some fundamental questions remain open and the correlation between the glass dynamics, the aging process and the alloy properties has not been well understood yet [17, 18]. For example, the frequency span and shape of the α-relaxation for different MGs are found to be quite similar by mechanical spectroscopy [1, 17], while the β-relaxation behavior depends rather sensitively on composition. Insights into these relations requires knowledge of the intrinsic physical processes on both the microscopic time and length scales. Over decades, this was hindered due to the lack of suitable complimentary techniques probing the corresponding microscopic dynamics in the time window of mechanical spectroscopy. Conventional dielectric spectroscopy and light scattering are not applicable due to the electrical conducting nature of alloys, and straightforward interpretation of nuclear magnetic resonance (NMR) measurements is only possible with a limited number of elements (isotopes), mostly those with relatively simple electron shell structures.

Study of the microscopic dynamics in metallic glasses

* fan.yang@dlr.de

has become feasible only recently with the instrumental developments of the X-ray photon correlation spectroscopy (XPCS) [16, 19–24]. XPCS directly probes the evolution of the structural relaxation features via monitoring the fluctuation of the scattered speckle pattern from a coherent X-ray beam. With the advances in the high brilliance third generation synchrotron sources, XPCS has emerged as a very powerful technique for studying microscopic dynamics, revealing unexpected phenomena like the intermittent, heterogeneous nature of the aging dynamics in metallic glasses [16]. With the use of a fast X-ray detector, here we determined intrinsic relaxation times in the range of $10^{-1} - 10^{4}$ s by XPCS, covering a large fraction of the time scales accessible by mechanical spectroscopy. Utilizing both techniques, we investigate structural relaxation processes on different length scales, and how the microscopic processes controls the macroscopic properties of the metallic glasses and supercooled melts.

II. EXPERIMENTAL PROCEDURE

XPCS and mechanical spectroscopy experiments were carried out on a well-known Zr-based BMG: $Zr_{46.8}Ti_{8.2}Cu_{7.5}Ni_{10}Be_{27.5}$, commercially known as Vitreloy® 4 (Vit4). Its undercooled melt exhibits a remarkable stability against crystallization, allowing the study of the supercooled liquid (SCL) region over a wide temperature range and long annealing times. Glassy ribbons of Vit4 were prepared from pure elements with a purity of at least 99.99% by arc-melting and subsequent melt spinning procedure under high purity argon atmosphere. During the melt spinning process the copper wheel linear tangential velocity was set to 40 m/s. The manufactured ribbons were 30±5 μm thick.

The XPCS measurement was carried out on the P10 beamline at the synchrotron facility PETRA III, DESY. The Vit4 ribbon was mounted on the standard P10 sample insert, between two copper plates which served both as mechanical support and thermal contact, and then placed into a DN100 vacuum cube evacuated down to better than 1×10^{-5} mbar. A coherent X-ray beam of 8.25 keV was used. Speckles patterns were collected by a EIGER X4M detector with a capability of frame rates up to 750 Hz placed at $\sim$ 1843 mm downstream of the sample, at a scattering angle of $2\theta = 36°$. This corresponds to a momentum transfer $q \sim 2.6$ Å^{-1}, i.e., at the position of the first structure factor maximum. A pre-annealing treatment before the XPCS experiment was performed to release the residual stress, by heating the ribbon up to 600 K using identical heating and cooling rates of 1 K/min, i.e., just above the calorimetric glass transition temperature T_g at this heating rate [25], with the ribbons clamped in straight shape. The sample was then measured in isothermal steps during two heating runs, one from 520 K to just above 600 K, and another from 520 K to 673 K [26]. A temperature incremental step of 5 K was used between the individual measurements for the SCL regime. Between the isothermal steps, 2θ scans were performed to confirm the amorphous nature of the ribbon. A temperature offset between the sample temperature and the furnace temperature of 27 K was corrected [27].

The mechanical relaxation behavior was investigated with mechanical spectroscopy and static stress relaxation experiments in a TA instruments Q800 Dynamic Mechanical Analyzer. The mechanical spectroscopy measurements were performed at a heating rate of 1 K/min with driving frequencies from 0.03 to 30 Hz. The static stress relaxation experiments were performed in isothermal steps applying constant strains of 0.1%. Before the application of the strain a 20 min isothermal equilibration was performed at each temperature. Similar to the XPCS measurements, also in both the stress relaxation and mechanical spectroscopy experiments, the ribbon was pre-annealed up to T_g before the measurements to reduce the internal stresses.

III. RESULTS

A. XPCS

In an XPCS experiment the quantitative information of the sample dynamics can be obtained by calculating the so-called two-time correlation function (TTCF)

$$G(q, t_1, t_2) = \frac{\langle I(q, t_1), I(q, t_2)\rangle_p}{\langle I(q, t_1)\rangle_p \langle I(q, t_2)\rangle_p}, \tag{1}$$

where $\langle \dots \rangle_p$ denotes an ensemble averaging over equivalent pixels corresponding to the same scattering vector q. A representative of TTCF of the ribbon in the SCL regime at 628 K is shown in Figure 1. For experiments which start at $t_1 = t_2 = 0$, its averaged $g^2(q, t)$ function at a mean time of $(t_1 + t_2)/2$ and a lag time $t = |t_1 - t_2|$, corresponds to

$$g^2(q, t) = 1 + \gamma(q)|f(q, t)|^2 \tag{2}$$

where $\gamma(q)$ is the q-dependent speckle contrast in the experiment and $f(q, t)$ is the intermediate scattering function. The scattering function reflects the time dependence of the density (electronic) correlation in the sample, which is a spatial Fourier transformation of the density auto-correlation function, and hence the atomic dynamics [28].

The common heterogeneous feature of structural relaxation is usually described according to the Kohlrausch-Williams-Watts (KWW) function, which gives

$$g^2(q, t) = 1 + a(q)\exp[-2(t/\tau(T))^{\beta(T)}] \tag{3}$$

where τ is the characteristic relaxation time, β is the shape parameter ($\beta < 1$ defines a stretched and $\beta > 1$ a compressed exponential decay). $a(q) = \gamma(q)f^2(q)$ is the

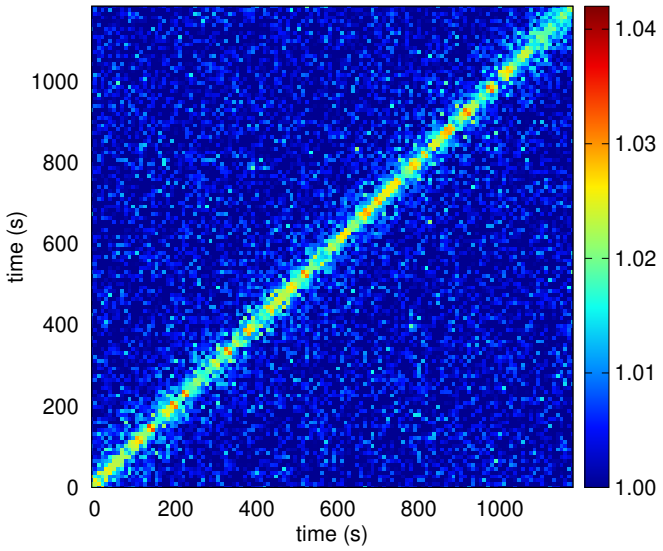

FIG. 1. Two-time correlation function (TTCF) measured on the Vit4 ribbon by XPCS at 628 K.

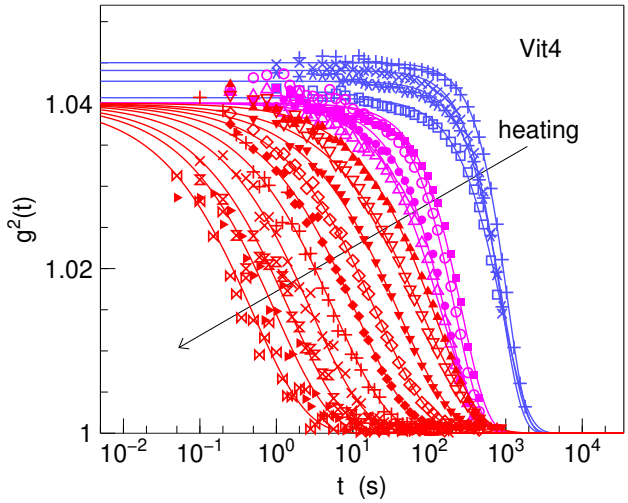

FIG. 2. Measured $g^2(t)$ functions on Vit4 ribbons. Temperatures from right to left: 523 K, 543 K, 553 K, 563 K, 583 K, 593 K, 598 K, 603 K, and from 613 K with a 5 K increment up to 658 K. Blue magenta, and red symbols represent $g^2(t)$ in the glassy, glass transition, and SCL regions, respectively.

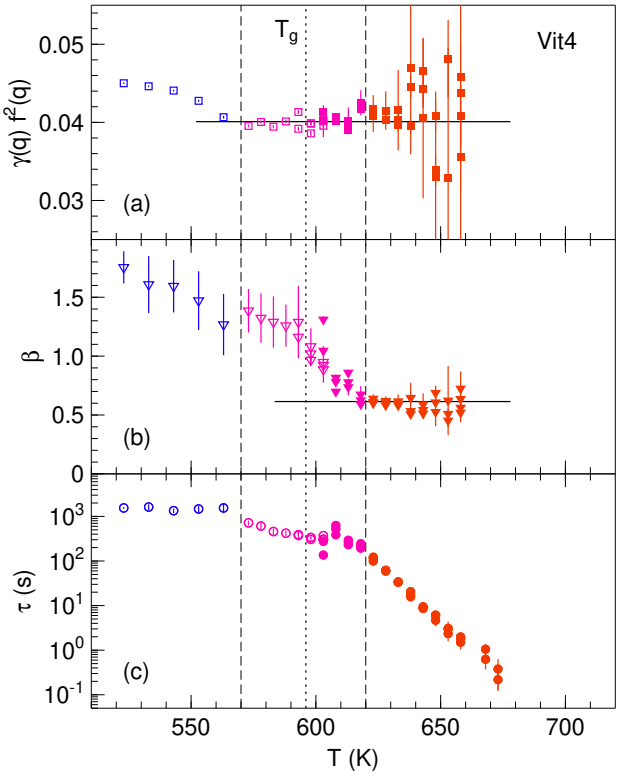

FIG. 3. Evolution of (a) the pre-exponential factor $a(q) = \gamma(q)f^2(q)$, (b) the stretching exponent β, and (c) the decay time τ of the obtained $g^2(t)$ function as a function of temperature. Open symbols correspond to data obtained in the 1st heating, full symbols correspond to that from the 2nd heating. Horizontal lines in (a) and (b) represents the average value of $a(q)$ and β in the SCL regime, respectively. The dashed vertical line marks the glass transition region. The calorimetric glass transition temperature at this heating rate is around 596 K [25] (dotted line). Same as in Fig 2, the blue, magenta, and red colors represent data obtained in the glassy, glass transition, and SCL regimes, respectively.

product of the speckle contrast $\gamma(q)$ and the so-called non-ergodicity parameter $f(q)$ (or Debye-Waller factor) [19]. Fig. 2 shows the measured $g^2(t)$ functions at different temperatures. Since all measurements here were done at a single scattering vector q, we dropped the q notation of the correlation function in the following. Without further notice, this refers always to $q = 2.6\,\text{Å}^{-1}$ i.e., at the first structural factor maximum. For clarity some temperatures are omitted in the plot. From right to left the measurement temperature increases. Consequently the dynamics become faster and the characteristic timescale on which the correlation function $g^2(t)$ decays decreases.

The solid lines in Fig. 2 represent the best fit of the measured $g^2(t)$ according to eq. 3. The fitting procedure was done in an iterative way: first all fit parameters were free adjustable during fitting. This gives a pre-exponential factor $a(q)$ which decreases with increasing temperature below 573 K, and then scatters around a value $a(q) \sim 0.04$ above 573 K, as shown in Fig 3a. Above 630 K the uncertainty is considerably larger as the initial decay of $g^2(t)$ is moving out of the accessible time window due the faster dynamics at higher temperatures. In a second step for temperatures above 573 K the a is set to 0.0401 (horizontal line in Fig. 3a). This results in shape parameter β displayed in Fig 3b. It can be seen that the β exhibits a continuous decrease with increasing temperature up to of about 620 K, then it remains almost temperature independent with a value of about 0.61. The structural relaxation time τ is hence derived accordingly with a fixed $a = 0.0401 \pm 0.0005$ above 573 K and with additionally a fixed $\beta = 0.61 \pm 0.04$ above 620 K.

In Fig. 3 we also distinguished data obtained during

the first and second heating and shown fit parameters derived from different exposure times. It can be seen that the parameters obtained from the second heating are a continuation of that obtained from the first heating. The results are in agreement within error bars in the overlapping region. The measured $g^2(t)$s agree also between different detector exposure times, with the only difference that at short exposure time the signal-to-noise ratio decreases. Hence, although the Eiger detector used in the experiment is capable to be operated at even higher frame rates, we did not explore the $g^2(t)$ details below 0.1 s.

B. Mechanical relaxation

The stress relaxation is observed by recording the decay of stress change with time. The evolution of the stress, normalized to the initial value, at different temperatures is shown in Fig. 4a. Similar to the XPCS measurement, here the decay of the stress can be described by a stretched exponential

$$\sigma(t)/\sigma_0 = \exp[-(t/\tau)^{\beta}], \qquad (4)$$

where τ is the timescale of the stress relaxation, β is the stretching KWW exponent, and σ_0 is the initial applied stress. With this we assume that also in the glassy region the applied stresses can be fully relaxed. A similar fitting procedure for determining the stretching exponent was used: below 620 K β was left as a free fitting parameter, and above 620 K a fixed $\beta = 0.525$ was used. The characteristic relaxation timescale is then derived accordingly.

The obtained relaxation time and shape parameter are shown in Fig. 4b and Fig. 4c as a function of temperature. In contrast to $g^2(t)$ in the XPCS experiment, in the glassy region the shape of the stress relaxation curve remains stretched, with a stretching exponent β slightly below 0.5. This increases across the glass transition, here observed around 600 K, towards an average, constant value of $\beta \sim 0.5$. The transition temperature can be also consistently identified from where the obtained relaxation time changes its temperature dependence. In addition to the stress relaxation experiments, the α peak of the loss modulus was obtained from mechanical spectroscopy at different frequencies, and fitted to the Havriliak-Negami function in order to obtain the corresponding relaxation time and shape parameters [29]. The relaxation times of the α peak, shown in Fig. 4c, are in agreement to that obtained from the static stress relaxation above T_g, while below the glass transition they diverge due to the different aging state of the samples used in the two types of probes. The mechanical spectroscopy measurements were performed at a constant heating rate of 1 K/min while the stress relaxations were monitored in long isothermal steps, mimicking the thermal protocol in the XPCS experiments.

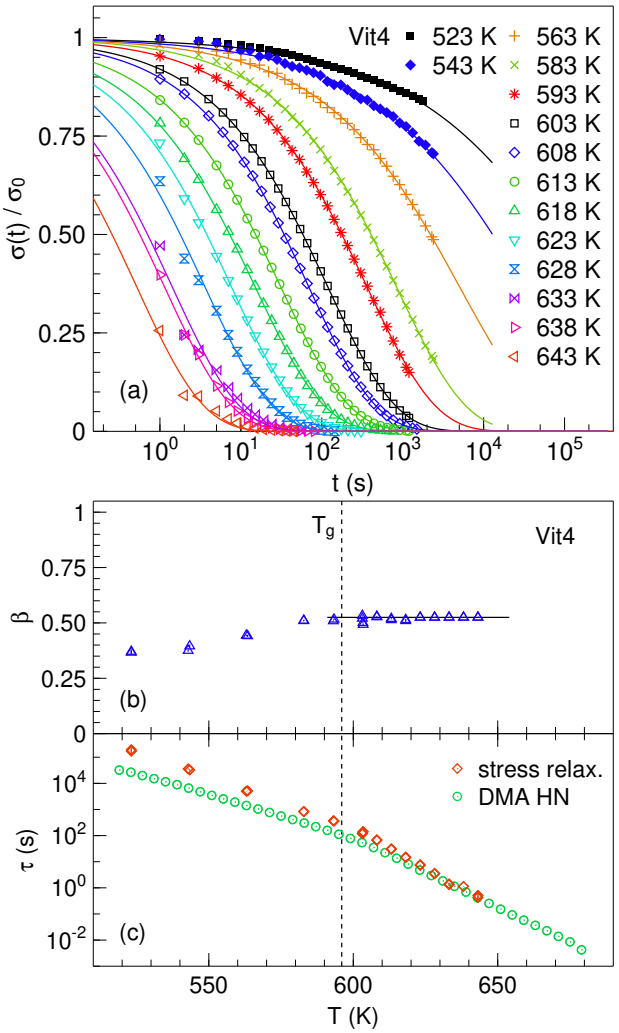

FIG. 4. (a): Decay of the normalized stress measured at constant strain steps at different temperatures on the Vit4 sample. (b) and (c): Derived stretching exponent and relaxation times according to eq. 4, respectively. In (c) also the relaxation times of the α-peak obtained from the mechanical spectroscopy measurements are shown. Dotted line represents the temperature of the calorimetric glass transition.

IV. DISCUSSION

A. Behavior across the glass transition

As shown in Fig 3 upon heating across the glass transition the shape of the $g^2(t)$ function changes from a compressed ($\beta > 1$) to a stretched shape ($\beta < 1$). Also a drop of the non-ergodicity parameter $f(q)$ is observed, as the scattering contrast $\gamma(q)$, although depends on the experimental set-up, can be regarded as temperature independent within the studied temperature range. This is consistent with the previous observation on MGs with XPCS, in particular, the change from the compressed to stretched $g^2(t)$ upon an entry into the supercooled liquid region [19, 30].

Moreover, here we are able to show that for Vit4 across the glass transition there is a continuous, monotonic change in both β and $f^2(q)$: $f^2(q)$ decreases with increasing temperature until 570 K, and then becomes almost temperature independent within the experimental uncertainty. Also the β value drops continuously from 1.75±0.14 at 523 K to 0.67±0.07 at 618 K. β <1 indicates that the sample has reached the supercooled liquid state [16, 19], inline with where the relaxation time τ exhibits a different slope or activation energy (Fig. 3c). The transition occurs during the heating experiment starting around 600 K, at this temperature β falls below 1, and culminates around 618 K, with a relaxation timescale of about 245 s.

On the other hand, below 570 K $f^2(q)$ decreases continuously upon heating towards an almost constant value in the supercooled liquid region. Such a temperature dependence of $f^2(q)$ is very similar to the change of the Debye-Waller factor observed in metallic and non-metallic glasses due to a fast (β) relaxation process, for which the mode coupling theory (MCT) predicts [31]

$$f(q) = f^c(q) + h_c\sqrt{(T_c - T)/T_c} \qquad (5)$$

where T_c is the critical temperature of the MTC, $f^c(q)$ is the Debye-Waller factor at T_c, and h_q is an amplitude. However, it is obvious that here this plateau value is reached even below the glass transition temperature T_g, and T_c = 875 K of the Vit4 alloy is considerably higher [13]. Thus, despite the similar temperature dependence, the standard MCT scenario does not apply. Certainly a fast relaxation processes upon entering the SCL would be an intuitive interpretation. Yet, the characteristic transition temperature and timescale depends both on the wave number and on the experimental observation time window. Thus, they are not directly comparable with those observed by other experimental techniques. For example, in the neutron back-scattering and the Mössbauer absorption experiments the observed $f(q)$ of Vit4 is completely harmonic in this temperature range [25, 32]. Moreover, below T_g the sample is a stiffer material and the dynamics observed by XPCS could always be a superposition of possible (residual) stress-driven dynamics and the intrinsic relaxation dynamics. Additional studies, particularly focusing on the short timescale dynamics, are needed to clarify their effect, before the drop of $f^2(q)$ can be unambiguously attributed to the intrinsic β-relaxation.

The presence of compressed microscopic dynamics has been observed in a variety of out-of-equilibrium systems, jammed soft materials [33–35]. In the case of soft glasses, the compressed dynamics has been associated to dipole forces due to a stress field occurring in the out-of-equilibrium state. This is related to the densification during aging, which creates some micro-collapses leading to a ballistic-like collective particle motion. Here in Vit4, beside the common β ∼1.5 shape exponent, the observation of a continuous, monotonic decrease of beta across the glass transition appears to be very similar to these soft disordered systems, which has not been reported previously in metallic glasses. This behavior suggests the existence of a progressive transition between the stress-dominated dynamics of glasses and the mixed diffusion and hopping particle motion of supercooled alloys [23]. Nevertheless, with respect to the case of soft glassy materials, the detailed microscopic picture in MGs remains to be disclosed, due to the difficulty to probe the intermediate scattering function in a glass below T_g with both others experimental techniques and numerical simulations. Only very recently, numerical works have shown the compressed correlation functions in the self-part of the intermediate scattering function in metallic glass formers, attributed to the increasing connectivity in icosahedral clusters upon cooling in the supercooled liquid state [36].

B. Time-temperature-superposition above T_g

Fig. 5 shows the $g^2(t)$ function obtained by XPCS and the decay of the normalized stress $\sigma(t)/\sigma_0$ for the SCL regime, both scaled with the corresponding relaxation time in the temperature range between 603 K an 658 K. It can be seen that after the scaling, both $g^2(t)$ and $\sigma(t)/\sigma_0$ fall onto a single master curve. A fit with a stretched exponential decay gives $\beta = 0.59 \pm 0.08$ for XPCS measurements and $\beta = 0.51 \pm 0.01$ for the mechanical relaxation, respectively. This is in agreement with the averaged value for β obtained in the previous section for the supercooled liquid region. Thus, in the entire SCL temperature range studied here, the atomic dynamics and the macroscopic stress relaxation are in full accordance with the time temperature superposition principle. The time temperature superposition properties for relaxation measured by mechanical spectroscopy are well known for metallic glasses in the supercooled liquid regime close to T_g [1, 17]. In fact, as shown in Fig. 5c, also in the frequency domain the loss modulus can be scaled onto a single master curve described by the imaginary part of the Havriliak-Negami function

$$E(\omega)/E_0 = 1 - \frac{1}{[1 + (i\omega\tau)^\alpha]^\gamma}, \qquad (6)$$

with $\alpha = 0.836 \pm 0.006$ and $\gamma = 0.405 \pm 0.006$, corresponding to a stretching exponent β of about 0.5 [29], which is rather universal for the α-relaxation in metallic glasses [37, 38].

Compared to the relaxation of mechanical stress, the $g^2(t)$ function obtained from XPCS exhibit a slightly higher β. However, it is within the uncertainty margin of the experiment. $\beta < 1$ is usually regarded as the result of a distribution of different relaxation times [7], associated with the presence of spatial and dynamical heterogeneity [39–42]. The slightly different stretching exponents observed in mechanical relaxation and in XPCS could be originated from the different relaxational observables

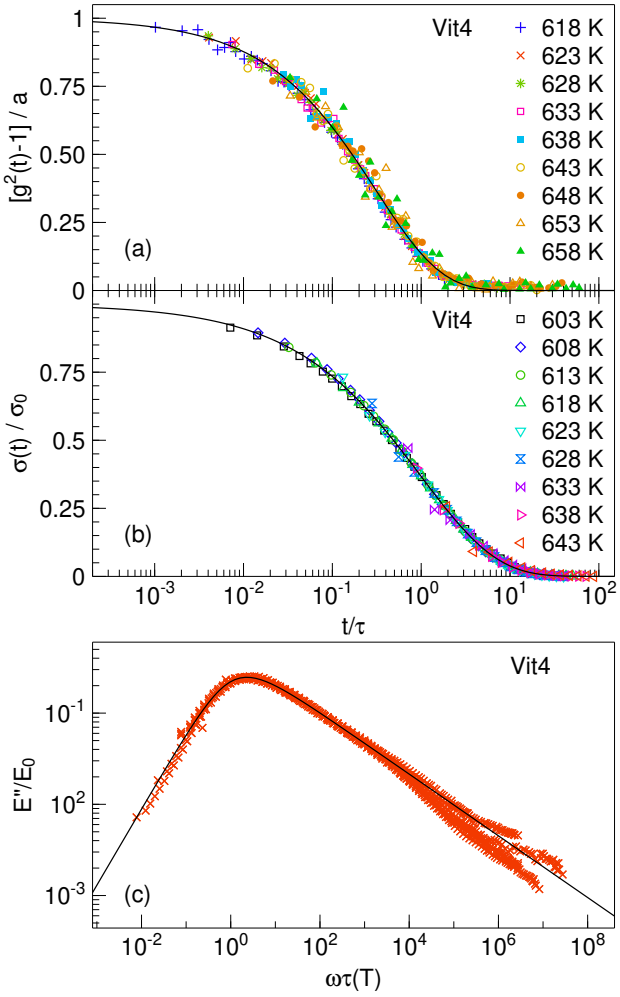

FIG. 5. Time-temperature superposition of the $g^2(t)$ function (a), normalized stress relaxation (b), and the normalized loss modulus (c) in the supercooled liquid regime of Vit4.

(stress vs. density correlations) probed in the two techniques.

C. Relaxation on different length scale

Fig. 6 shows the different relaxation times in the studied temperature range. The relaxation time (frequency) of the small Be atoms obtained by previous NMR study [43], and the equilibrium melt viscosity close to T_g [44] are also shown for comparison. The dashed line represents a Vogel-Fulcher-Tammann (VFT) fit of the melt viscosity, $\eta(T) = \eta_0 \exp[D^* T_0/(T - T_0)]$, where $\eta_0 = 4 \times 10^{-5}$ Pa s is the high temperature limit of the melt viscosity, D^* is the fragility parameter of the melt, and T_0 is the temperature where the barriers for the viscous flow become infinite. The fragility of the melt in this temperature range derived from the melt viscosity is of about 22.7 [44].

It can be seen that the relaxation time of Be atoms is

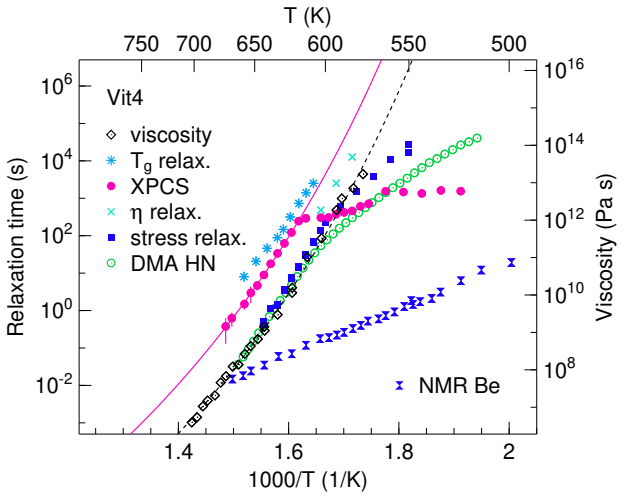

FIG. 6. Comparison of the microscopic and macroscopic relaxation time measured by XPCS, stress relaxation, and the peak of the loss modulus (DMA HN) of the Vit4 glass as a function of temperature. The viscosity of the supercooled melt [44] and Be atom relaxation time [43] are also shown. The solid and dashed lines represent VFT-fit of the XPCS relaxation time and the melt viscosity in the SCL, respectively. Star and cross symbols show the relaxation time obtained from heating rate dependent calorimetric T_g and from viscosity relaxation, respectively.

considerably faster and exhibits a different temperature dependence compared to those obtained from mechanical spectroscopy and XPCS. It has been previously observed that the small atom dynamics and the β-relaxation processes in a number of MGs, including Vit4, exhibit similar time scales and activation energies [45, 46]. However, in the temperature range investigated here, its time scale would be largely outside the observation time window of the XPCS measurement. In addition, for the Vit4 alloy, the correlation function measured by XPCS is dominated by the scattering that arises from the Zr atoms, due to its highest concentration and atomic number. Thus, the structural dynamics observed here by XPCS can be reasonably attributed to the α-relaxation, contributed mainly by the Zr atom dynamics.

In contrast to the decoupled small atom dynamics, the α-relaxation time τ_α obtained by mechanical spectroscopy and by XPCS exhibit very similar temperature dependence. The fragility parameters obtained from XPCS and stress relaxation times are 21.8±5.7 (solid line in Fig. 6) and 19.8±3.6, respectively. This agrees with that of the melt viscosity within the experimental uncertainty. This confirms that the relaxation time of the $g^2(t)$ function corresponds to the timescale of the α-relaxation. It is also known from previous measurements by Busch et al.[44] that the time required for the apparent viscosity to relax towards its equilibrium value during isothermal three point beam bending viscosity measurements, and the timescale derived from the heating rate dependent glass transition temperature are proportional

to the melt viscosity, as shown in Fig. 6. Thus, in the supercooled liquid regime investigated here, the structural relaxation is governed by a dominant microscopic relaxation timescale, which controls the macroscopic flow, the calorimetric glass transition, and the mechanical behavior. This is further supported by the similar stretching exponents.

Beside the similar stretching exponent and temperature dependence, however, the absolute timescale differs by of about a factor of 10 between the microscopic structural relaxation and the decay of the macroscopic stress. The temperature uncertainty in the different experimental techniques has been checked by various methods and cannot explain the difference in timescales. This should be also distinguished from the situation around 600 K observed previously for $Zr_{44}Ti_{11}Ni_{10}Cu_{10}Be_{25}$ [21], where similar relaxation times were found but, in the case of XPCS, the temperature dependence and the stretching exponent clearly corresponded to that in the glass transition region and hence different from that observed here in the SCL.

Such kind of discrepancies of relaxation times in the SCL are known for different physical quantities [18, 47, 48], also here shown for the heating rate dependent glass transition and the equilibrating time of the apparent viscosity in Fig. 6. Concerning the difference between the microscopic structural relaxation and macroscopic stress relaxation times, for Vit4, a *slower* microscopic relaxation time indicates that the stress can be already relaxed without a complete decay of the atomic correlation at next-nearest neighbor distances. Considering the highly collective nature of the atomic motion in the supercooled liquid, such scenario is not unphysical. The exact ratio between the timescales observed in XPCS and in stress relaxation, however, should reflect how the relaxation of stress is achieved by the mass transport, and depends on the detailed structural dynamics of the melt/glass, e.g.: the dynamics modes involved, and the number of atoms which are participating. In the Mg-Cu-Y glass, for instance, such discrepancy is considerably smaller [19]. Thus, this is a fundamental point still to be surveyed on a larger range of alloy systems and wave vectors q [23].

V. CONCLUSION

To summarize, in this study we emphasize the ability of measuring microscopic, intrinsic relaxation time with XPCS down to sub-second scale, covering a significant portion of the experimental accessible timescale of mechanical spectroscopy. With this, we compared the microscopic and macroscopic structural relaxation behavior of a bulk metallic glass forming alloy $Zr_{46.8}Ti_{8.2}Cu_{7.5}Ni_{10}Be_{27.5}$ in the supercooled liquid regime. We show that upon heating the onset of the supercooled liquid exhibits a continuous decease of the non-ergodicity parameter $f^2(q)$ and stretching exponent β of the intermediate scattering function. In the supercooled liquid, both the microscopic and macroscopic relaxations exhibit a time temperature superposition, with rather similar stretching exponents. In addition, a very similar temperature dependence of the two relaxation times are found, which agree with that of the melt viscosity in the investigated temperature range. This shows that the macroscopic flow and mechanical properties are controlled by the microscopic structural relaxation, with a dominant intrinsic timescale of the majority component, in our case Zr, common for these densely packed systems.

ACKNOWLEDGMENTS

We thanks Nico Neuber for helpful discussions. N.A. acknowledges the financial support from the German Academic Exchange Service (DAAD) via the DLR-DAAD special program. We acknowledge DESY (Hamburg, Germany), a member of the Helmholtz Association HGF, for the provision of experimental facilities.

[1] W. H. Wang, Prog. Mater. Sci. , 100561 (2019).
[2] C. A. Angell, K. L. Ngai, G. B. McKenna, P. F. McMillan, and S. W. Martin, J. Appl. Phys. **88**, 3113 (2000).
[3] J. C. Dyre, Rev. Mod. Phys. **78**, 953 (2006).
[4] E. Donth, *Relaxation and Thermodynamics in Polymers: Glass Transition* (Wiley, Berlin, 1992).
[5] H. Sillescu, J. Non-Cryst. Solids **243**, 81 (1999).
[6] T. Wang, J. Li, Y. Yang, and G. Rao, Intermetallics **19**, 81 (2011).
[7] C. Liu, E. Pineda, and D. Crespo, Metals **5**, 1073 (2015).
[8] J. Schroers, Adv. Mater. **22**, 1566 (2010).
[9] M. Chen, NPG Asia Mater. **3**, 82 (2011).
[10] J. J. Kruzic, Adv. Eng. Mater. **18**, 1308 (2016).
[11] Y. Sun, A. Concustell, and A. L. Greer, Nat. Rev. Mats. **1**, 16039 (2016).
[12] M. A. Gibson, N. M. Mykulowycz, J. Shim, R. Fontana, P. Schmitt, A. Roberts, J. Ketkaew, L. Shao, W. Chen, P. Bordeenithikasem, J. S. Myerberg, R. Fulop, M. D. Verminski, E. M. Sachs, Y.-M. Chiang, C. A. Schuh, A. John Hart, and J. Schroers, Mater. Today **21**, 697 (2018).
[13] A. Meyer, J. Wuttke, W. Petry, O. G. Randl, and H. Schober, Phys. Rev. Lett. **80**, 4454 (1998).
[14] F. Yang, T. Unruh, and A. Meyer, EPL (Europhysics Letters) **107**, 26001 (2014).
[15] C. Liu, E. Pineda, D. Crespo, J. Qiao, Z. Evenson, and B. Ruta, Journal of Non-Crystalline Solids **471**, 322 (2017).
[16] Z. Evenson, B. Ruta, S. Hechler, M. Stolpe, E. Pineda, I. Gallino, and R. Busch, Phys. Rev. Lett. **115**, 175701 (2015).

[17] J. Qiao, Q. Wang, J. Pelletier, H. Kato, R. Casalini, D. Crespo, E. Pineda, Y. Yao, and Y. Yang, Prog. Mater. Sci. **104**, 250 (2019).

[18] K. L. Ngai, *Relaxation and Diffusion in Complex Systems* (Springer, New York, 2011).

[19] B. Ruta, Y. Chushkin, G. Monaco, L. Cipelletti, E. Pineda, P. Bruna, V. M. Giordano, and M. Gonzalez-Silveira, Phys. Rev. Lett. **109**, 165701 (2012).

[20] B. Ruta, V. Giordano, L. Erra, C. Liu, and E. Pineda, J. Alloy Compd. **615**, S45 (2014).

[21] Z. Evenson, A. Payes-Playa, Y. Chushkin, M. di Michiel, E. Pineda, and B. Ruta, J. Mater. Res. **32**, 2014–2021 (2017).

[22] A. Das, P. M. Derlet, C. Liu, E. M. Dufresne, and R. Maaß, Nature Communications **10**, 5006 (2019).

[23] B. Ruta, S. Hechler, N. Neuber, D. Orsi, L. Cristofolini, O. Gross, B. Bochtler, M. Frey, A. Kuball, S. S. Riegler, M. Stolpe, Z. Evenson, C. Gutt, F. Westermeier, R. Busch, and I. Gallino, Phys. Rev. Lett. **125**, 055701 (2020).

[24] P. Luo, M. X. Li, H. Y. Jiang, R. Zhao, F. Zontone, Q. S. Zeng, H. Y. Bai, B. Ruta, and W. H. Wang, Phys. Rev. B **102**, 054108 (2020).

[25] A. Meyer, J. Wuttke, W. Petry, A. Peker, R. Bormann, G. Coddens, L. Kranich, O. G. Randl, and H. Schober, Phys. Rev. B **53**, 12107 (1996).

[26] A cooling step from 603 K to 520 K was performed in between.

[27] Based on the crystallization temperature of different alloy compositions at a heating rate of 1 K/min.

[28] A. Madsen, R. L. Leheny, H. Guo, M. Sprung, and O. Czakkel, New J. Phys. **12**, 055001 (2010).

[29] F. Alvarez, A. Alegria, and J. Colmenero, Phys. Rev. B **44**, 7306 (1991).

[30] X. D. Wang, B. Ruta, L. H. Xiong, D. W. Zhang, Y. Chushkin, H. W. Sheng, H. B. Lou, Q. P. Cao, and J. Z. Jiang, Acta Mater. **99**, 290 (2015).

[31] W. Götze and L. Sjögren, Rep. Prog. Phys. **55**, 241 (1992).

[32] A. Meyer, H. Franz, B. Sepiol, J. Wuttke, and W. Petry, Europhys. Lett. **36**, 379 (1996).

[33] L. Cipelletti, S. Manley, R. C. Ball, and D. A. Weitz, Phys. Rev. Lett. **84**, 2275 (2000).

[34] L. Cipelletti, L. Ramos, S. Manley, E. Pitard, D. A. Weitz, E. E. Pashkovski, and M. Johansson, Faraday Discuss. **123**, 237 (2003).

[35] P. Ballesta, A. Duri, and L. Cipelletti, Nat. Phys. **4**, 550 (2008).

[36] Z. W. Wu, W. Kob, W.-H. Wang, and L. Xu, Nat. Comm. **9**, 5334 (2018).

[37] L. M. Wang, R. Liu, and W. H. Wang, J. Chem. Phys. **128**, 164503 (2008).

[38] J. C. Qiao and J. M. Pelletier, J. Alloy Compd. **589**, 263 (2014).

[39] L. Berthier, G. Biroli, J.-P. Bouchaud, L. Cipelletti, and W. van Saarloos, eds., *Dynamical Heterogeneities in Glasses, Colloids, and Granular Media* (Oxford University Press, New York, 2011).

[40] M. D. Ediger, C. A. Angell, and S. R. Nagel, J. Chem. Phys. **100**, 13200 (1996).

[41] M. D. Ediger, Ann. Rev. Phys. Chem. **51**, 99 (2000).

[42] E. R. Weeks, Science **287**, 627 (2000).

[43] X.-P. Tang, U. Geyer, R. Busch, W. L. Johnson, and Y. Wu, Nature **402**, 160 (1999).

[44] R. Busch, E. Bakke, and W. Johnson, Acta Mater. **46**, 4725 (1998).

[45] H.-B. Yu, W.-H. Wang, and K. Samwer, Materials Today **16**, 183 (2013).

[46] I. Gallino and R. Busch, JOM **69**, 2171 (2017).

[47] G. Wilde, Applied Physics Letters **79**, 1986 (2001).

[48] Y. Liu, T. Fujita, D. Aji, M. Matsuura, and M. W Chen, Nat. Comm. **5**, 3238 (2014).